POTENTIAL CLINICAL RELEVANCE

Nanomedicine: Nanotechnology, Biology, and Medicine
9 (2013) 550–557

Original Article

nanomedjournal.com

Radiative-surface plasmon resonance for the detection of apolipoprotein E in medical diagnostics applications

Beniamino Sciacca, PhD[a,*], Alexandre François, PhD[a], Manuela Klingler-Hoffmann, PhD[b], Julie Brazzatti, PhD[b], Megan Penno, PhD[b], Peter Hoffmann, PhD[a,b], Tanya M. Monro, PhD[a]

[a]*Institute for Photonics and Advanced Sensing, School of Chemistry and Physics, The University of Adelaide, Adelaide, SA 5005, Australia*
[b]*Adelaide Proteomics Centre, School of Molecular and Biomedical Science, The University of Adelaide, Adelaide, SA 5005, Australia*

Received 28 March 2012; accepted 27 October 2012

Abstract

Surface plasmon resonance (SPR)-based sensors enable the rapid, label-free and highly sensitive detection of a large range of biomolecules. We have previously shown that, using silver-coated optical fibers with a high surface roughness, *re-scattering* of light from the surface plasmons is possible, turning SPR into a radiative process. The efficacy of this platform has proven for the detection of large biomolecules such as viruses, proteins and enzymes. Here, we demonstrate that by bringing together this novel emission-based fiber SPR platform with an improved surface functionalization process aimed at properly orienting the antibodies, it is possible to rapidly and specifically detect the regulation of human apolipoprotein E (apoE), a low-molecular-weight protein (~39 kDa) known to be involved in cardiovascular diseases, Alzheimer's disease and gastric cancer. The results obtained clearly show that this new sensing platform has the potential to serve as a tool for point-of-decision medical diagnostics.

From the Clinical Editor: In this study, a novel emission-based surface plasmon resonance platform using silver-coated optical fibers is described. Properly orienting antibodies on the surface enables rapid and specific detection of human apolipoprotein E (apoE).

Key words: Surface plasmon resonance; Biosensor; Apolipoprotein E; Gastric cancer; Surface functionalization

Surface plasmons are electromagnetic waves at the interface of two media that have permittivity with opposite signs, as in the case of a metal and a dielectric.[1] Surface plasmons can be excited using a prism-based configuration (Kretschmann and Otto configuration),[2] via a waveguide-based approach,[3] or a fiber-based architecture.[4,5] All of these approaches exploit the evanescent field at the substrate–metal interface, which resonantly interacts with plasmons–polaritons at the metal–dielectric interface.[6] Surface plasmon resonance (SPR) is sensitive to changes of refractive index of the dielectric, and thus can be applied as a powerful technique for biosensing.[7] In the case of a prism-based configuration, the resonance is monitored by collecting the reflected light as a function of the incidence angle (at a fixed wavelength) or as a function of the incident wavelength at a fixed angle.[8] In waveguide or optical fiber architectures, a broadband light source is used to excite the surface plasmons, and the transmitted light is collected and analyzed to monitor the resonance, which appears as a dip in the spectrum.[1]

We have previously demonstrated that the plasmonic wave's energy can be scattered when a rough metallic film is used and re-emitted as light, turning SPR it into a radiative process.[9] In particular we have shown that the re-scattered light from a silver-coated optical fiber could be used efficiently as a biosensing platform to detect the influenza A virus. The platform offers many advantages to more conventional SPR architectures, such as a higher signal-to-noise ratio, the possibility to perform fluorescence and SPR simultaneously within the same device, and the possibility of having a reference channel on the same fiber for reducing environmental drifts that could affect the reliability of the device.

One challenge that faces all SPR-based sensors is that they work best for large molecules, as in such cases a relatively small number of molecules is required to observe a change in the SPR response, and we have previously shown that influenza A virus (thousands of kDa) is easily detected by the radiative-SPR platform.[9]

The authors acknowledge the support of an NHMRC Project Grant. T. Monro acknowledges the support of an ARC Federation Fellowship.

*Corresponding author: Institute for Photonics and Advanced Sensing and School of Chemistry and Physics, The University of Adelaide, North Terrace, Adelaide, SA 5005, Australia.

E-mail address: beniamino.sciacca@adelaide.edu.au (B. Sciacca).

1549-9634
http://dx.doi.org/10.1016/j.nano.2012.10.007

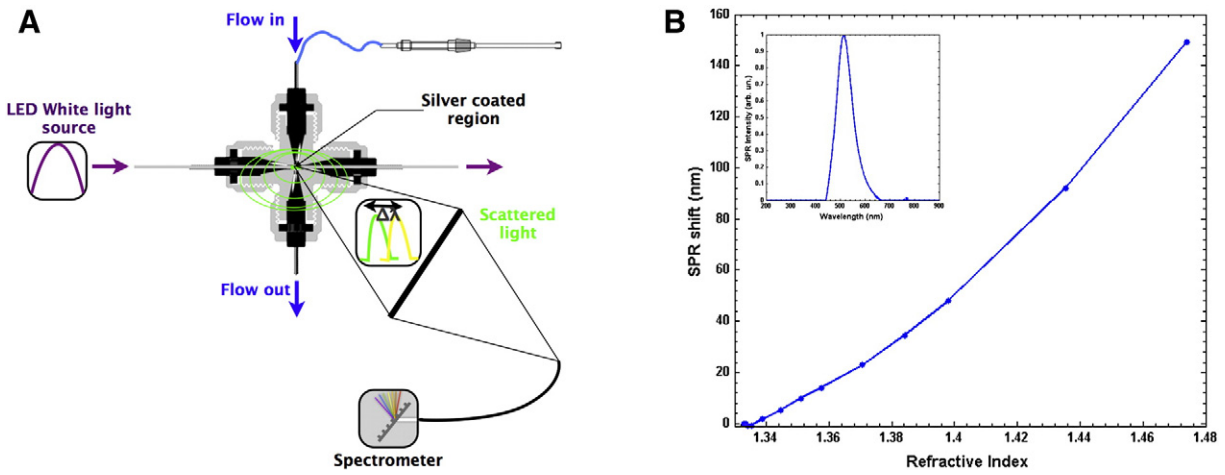

Figure 1. **(A)** Representation of the surface plasmon resonance biosensing architecture: the re-scattered plasmonic wave from the silver-coated optical fiber is collected and analyzed using a compact spectrometer. **(B)** Measured SPR response shift versus bulk index of refraction of the water/glycerol solutions in contact with the silver SPR probe surface. Inset shows a typical measurement of the re-scattered SPR signal.

In this article we explore the role surface functionalization plays not only in ensuring the specificity of the sensor, but in improving the detection limit and enabling it to sense relatively small proteins. In addition, we present some improvements to the sensor architecture, including the use of an LED source and a simplified flow cell. Comparing two different approaches for immobilizing the antibodies on the surface of the sensor, we demonstrate that the detection limit can be reduced if the antibodies are properly oriented, enabling efficient sensing and quantification of relevant concentration of human apoE, a relatively low-molecular-weight (~39 kDa) protein, known to be one of the major determinants in lipid transport, playing a critical role in arteriosclerosis and other diseases including Alzheimer's disease.[10,11] The same protein is also indicated as potential biomarker in gastric cancer,[12,13] where a significant up-regulation of apoE mRNA occurs in patients presenting the disease. Conventional methods for detecting apoE, such as enzyme-linked immunosorbent assay (ELISA), are expensive in terms of equipment needed to perform the analyses. In particular, commercially available ELISA kits used to quantify apoE concentrations take about 5 h before reaching a readable signal (see technical notes from Mabtech about "*ELISA for Human Apolipoprotein E*," http://www.mabtech.com).

Methods

Sensor fabrication

The SPR sensor was fabricated as reported in François et al.[9] Briefly, it was fabricated from a bare core (unstructured) optical fiber made of F2 Schott lead silicate glass with a refractive index of 1.62 and a diameter of 130 μm. The fiber was produced in-house by extruding a bulk glass sample into a rod and drawing into a fiber by using a fiber drawing tower. The fiber was subsequently coated with a polymer with a refractive index of 1.52. A short section (~4 mm) of the coating was mechanically stripped and coated with silver using the Tollens reaction.[14] A solution of 20 mL of $AgNO_3$ 0.24 mol/L and 40 μL of KOH 0.25 mol/L was reacted with a 20-mL mixture of methanol and glucose (1.9 mol/L) 1:2, in a petri dish in the presence of the fibers for 8 min at room temperature. After the coating, the fibers were thoroughly rinsed in millipore water and dried in air. The sensors were then immersed for 30 min in a 2-mg/mL solution of poly(allylamine hydrochloride) (PAH), a positively charged polyelectrolyte that adsorbs onto the negatively charged silver surface, introducing amine groups for further bioconjugation, rinsed with millipore water and dried under a stream of nitrogen.

Flow cell

Silver-coated fibers were mounted in a flow cell to expose the sensor to different species under controlled flow conditions. The flow cell used was adapted from the commercial IDEX MicroCross product, by drilling a 600-μm hole from the top of the piece to allow the collection of the light scattered by the sensor. A 600-μm glass rod placed into the hole was used to seal the flow cell. The flow cell was connected to a syringe by means of capillary tube with an internal diameter of 150 μm and a length of 5 cm. A syringe pump (Chemyx nanojet) connected to the syringe was used to control the flow rate of the species inside the flow cell. The total volume of the flow cell is in the order of microliters (see Figure 1, *A*).

Optical setup

Light from a white LED (6500K, Thorlabs) was focused and coupled into the fiber samples. In our previous work we used a broadband halogen light source,[9] now replaced with the white LED whose emission spectrum intensity is centered in the SPR wavelength region, reducing the background of the scattered signal overlapping that of the emitted SPR. To some extent, this increases the signal-to-noise ratio, thus improving the sensor resolution[15] and enabling a better detection limit. The light scattered out from the silver-coated region was collected directly from this region by focusing the light into a commercial optical fiber (Ocean Optics) positioned directly under the sensing area

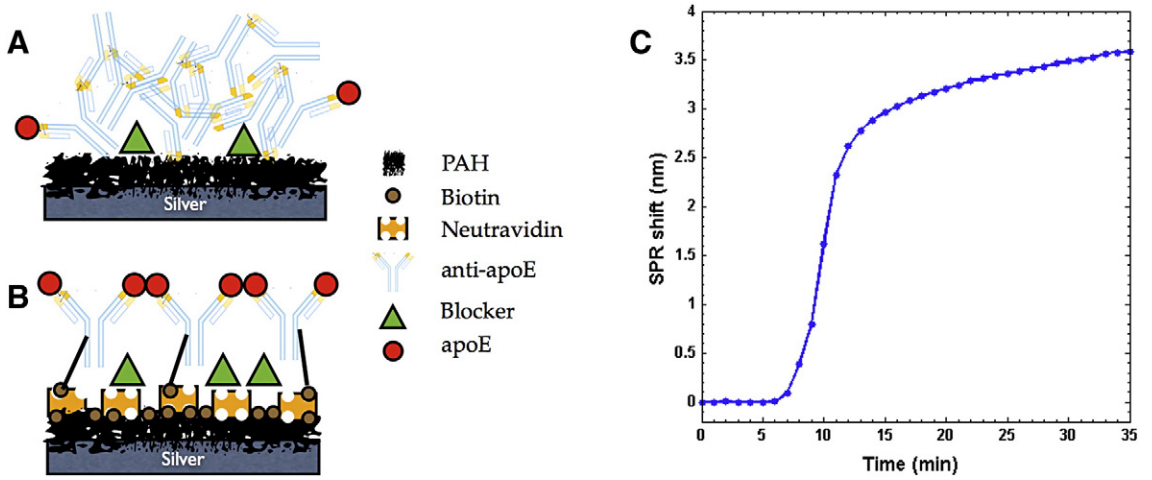

Figure 2. **(A)** Schematization of the *cross-linking* surface functionalization strategy: the antibodies are covalently linked to the polyelectrolyte layer. **(B)** Schematization of the *biotin–neutravidin* functionalization strategy explored in this work: biotinylated antibodies are linked to a neutravidin layer, enabling a proper orientation. **(C)** Typical real-time measured SPR response for neutravidin immobilization from a 400-nM solution.

and analyzed using a cooled spectrometer (Ocean Optics, QE65000) (see Figure 1, *A*). The inset in Figure 1, *B* shows a typical recorded spectrum for the re-scattered SPR signal from a sensor immersed in millipore water.

Data analysis

The recorded scattering spectra were analyzed by means of an in-house developed Matlab routine that performs a cross-correlation between the spectra, and identifies the wavelength of the cross-correlation signal by fitting with a single Gaussian curve. The SPR position was monitored in real time during the biosensing experiment, providing feedback during the surface functionalization procedures as well as during the biosensing measurements. The typical error in these measurements arises from the approximation of the curve to be fitted with a single Gaussian model, but the value obtained for the coefficient of determination approached the unity.

Adsorbate quantification

The quantification of biological species adsorbed on the sensor's surface is critical for the optimization of the surface functionalization and together with SPR spectroscopy enables to perform surface science studies, directly detecting adsorption onto a surface with submonolayer sensitivity. In particular, the adsorbate amount can be quantified from the SPR response, assuming the dielectric properties of the metal and of the adsorbate are known. The SPR response can be approximated as linear over a narrow range of refractive index[16]:

$$R = m(n_{\mathrm{eff}} - n_{\mathrm{s}}) \tag{1}$$

where m is the sensitivity, calculated from the slope of Figure 1, *B* for the range of interest (see Sensor characterization), n_{s} is the bulk solution refractive index and n_{eff} is the effective refractive index of the bilayer *adsorbate-bulk solution* on the sensor surface, where the thickness of the adsorbate layer is d_{a}. Since light is used to probe this index of refraction, it is straightforward to assume that the proper weighting factor at each point in the bilayer structure should be proportional to the intensity of light at that point. The evanescent electromagnetic field decays away exponentially into this medium with a characteristic decay length, l_{d}, of ~25% to 50% of the wavelength of the light.[17] From the SPR response, the effective refractive index of the liquid layer can be estimated, and used to estimate the penetration depth (l_{d}) of the evanescent field into the sensing region, which comes from Maxwell's equations[16]:

$$l_{\mathrm{d}} = \frac{\lambda}{2\pi Re\left\{-n_{\mathrm{eff}}^4/\left(n_{\mathrm{eff}}^2 + \varepsilon_{\mathrm{metal}}\right)\right\}^{\frac{1}{2}}} \tag{2}$$

where $\varepsilon_{\mathrm{metal}}$ is the complex dielectric constant of the metal at the SPR wavelength. l_{d} is an estimation of the interaction depth of the SPR with the sensing medium.

The adsorbate film thickness d_{a}, assuming it is small relative to l_{d}, could be calculated from the SPR response as follows[16]:

$$d = \frac{l_{\mathrm{d}}}{2}\frac{R}{m(n_{\mathrm{a}} - n_{\mathrm{s}})} \tag{3}$$

where n_{a} is the bulk refractive index of the adsorbate. From the effective adsorbate thickness and its molecular weight, the surface coverage (ng/cm^2) can be calculated[16]:

$$S_{\mathrm{C}} = 100 d_{\mathrm{a}} p_{\mathrm{a}} \tag{4}$$

where p_{a} is the bulk density of the adsorbate in g/cm^3. The quantification of the surface coverage for adsorbed/bound species on the sensor surface enables an estimate to be made of the quality of the functionalization approach and enables systematic optimization. The surface coverage was estimated for each step in the functionalization process and was used to compare the two functionalization approaches proposed here.

Surface functionalization approaches

Two different approaches for immobilizing anti-apoE antibodies on the surface were compared. In the first strategy (in the text named as *cross-linking* approach, see Figure 2, *A*), a 330 nM solution of antibody was used to link to the amine-terminated surface in presence of 0.22 M 1-ethyl-3-(3-dimethylaminopropyl) carbodiimide (EDC) and 0.22 M *N*-hydroxysuccinimide (NHS), reacting for 90 min, and the wavelength of the emitted SPR was monitored over time. Under these experimental conditions, the presence of the coupling agents activates any carboxylic group present on the antibodies creating a semi-stable amine-reactive NHS-ester that reacts with amine groups to form a stable amide bond.[18] After the immobilization of anti-apoE antibodies, the surface was blocked with a commercial blocking reagent ("The Blocking Solution," Candor) overnight to reduce non-specific binding, until no further shift in the SPR position was observed as a means of ensuring a complete saturation of the available functional group. The blocking reagent prevents non-specific binding occurring and is essential in label-free biosensing approaches, where the detection mechanism is based on the local change of refractive index caused by the presence of the mass of the analyte. After the passivation, the sensor was exposed to the analyte solution.

In the second approach (referred to here as the *biotin–neutravidin* strategy, see Figure 2, *B*), biotin (0.6 mg/mL), a vitamin containing a carboxylic group, was covalently bound to the amine-terminated surface of PAH in the presence of EDC (0.2 M) and NHS (0.2 M) for about 30 min, and the SPR signal was monitored over time. After a thorough PBS wash, the surface was exposed for about 40 min to a 400-nM solution of neutravidin, a tetrameric protein that binds specifically biotin, previously immobilized, forming a strong non-covalent bond ($K_D \sim 10^{-15}$ M).[19] After a thorough PBS wash, a 330-nM solution of biotinylated anti-apoE immunoglobulin (IgG) was flowed for about 90 min, allowing the biotin function of antibodies to bind to free groups on neutravidin, thanks to its tetrameric conformation. After the immobilization of antibodies, the sensor was exposed to the blocking solution overnight in order to block any unreacted binding site, preventing non-specific binding. As for the first approach, the exposure time of the species in the flow cell was varied until no further shift in the SPR position was observed as a means of ensuring a complete saturation of the available functional group.

Results

Sensor characterization

The performance of the sensor was characterized by exposing the sensing region of freshly coated sensors to glycerol/water solutions with refractive indices ranging from 1.33 to 1.47, and measuring the SPR response. Figure 1, *B* shows the measured shift in the SPR wavelength with respect to its position in water, as a function of the refractive index. From the data in Figure 1, *B*, it is possible to estimate the sensitivity of the system as a function of refractive index. Figure 1, *B* demonstrates that the sensitivity calculated as wavelength shift (S) increases with increasing refractive index, consistently with predictions.[6] For liquids with effective refractive indices in the range 1.3–1.4, which is relevant for aqueous environments in biological applications, the sensitivity of the sensor is approximately 740 nm/RIU, smaller than the best-reported values for fiber optics-based SPR sensors operating in this range.[16,20]

However, the limit of detection (LOD) is often reported as a mean to measure the performance of a sensor, although it is not an intrinsic characteristic of the sensor because it depends on the equipment used to measure it. In the case of our platform, the equipment and the data analysis we use, allow us to discriminate a SPR shift (R) of 0.03 nm, calculated as three times the noise.[21]

$$\mathrm{LOD} = \frac{R}{S} \tag{5}$$

The resulting LOD of our platform from Eq. 5 is 0.4×10^{-4} RIU. Such a LOD is not as good as the best-reported fiber-based SPR sensors,[20] but it is still comparable to other recently reported values for fiber-based SPR.[22,23] The reason for the poorer performance is the high refractive index of the glass substrate used here (1.62), which is larger than the commonly employed silica substrates (1.45). In fact, a lower refractive index of the substrate results in higher sensitivity.[24] Numerical simulations and experimental results we have obtained have demonstrated that a decrease of refractive index for the fiber substrate from 1.62 (F2 glass) to 1.45 (silica) results in a sensitivity increase of at least a factor 5 (data not shown), measured by collecting the scattered plasmonic wave. The use of lower index glasses offers a route to future improvement of the sensor performance, with a predicted LOD of at least 0.8×10^{-5} RIU, in the same order of magnitude of the best performing optical fiber-based SPR platform.[2,20]

However, quantitatively speaking, we do not expect the proposed architecture to have higher sensitivity respect to transmission-based optical fiber SPR platform, as the intrinsic sensitivity does not depend on the collection strategy. Some advantage of our architecture, compared to conventional transmission-based SPR is, as previously discussed in François et al[9] the improved SNR, the lower control needed on the metallic coating thickness, the higher versatility in terms of the possibility to perform fluorescence sensing based techniques such as completing a sandwich assay within the same platform and last but not least the capability of multiplexing, which is not possible with transmission based SPR on the same optical fiber.

As mentioned in Adsorbate quantification, the estimation of the sensor's sensitivity is required to enable quantification of the number of biomolecules immobilized on the surface, as explored further below.

Biotin–neutravidin immobilization

As described in Surface functionalization approaches, two different functionalization strategies were tested. In one strategy, IgGs were immobilized on the amine-terminated PAH layer by means of cross-coupling reagents. In the other functionalization approach, after covering the negatively charged silver film with the positively charged PAH polyelectrolyte, biotin was covalently linked to the free amine groups on PAH, as reported in Surface functionalization approaches neutravidin, a deglycosylated

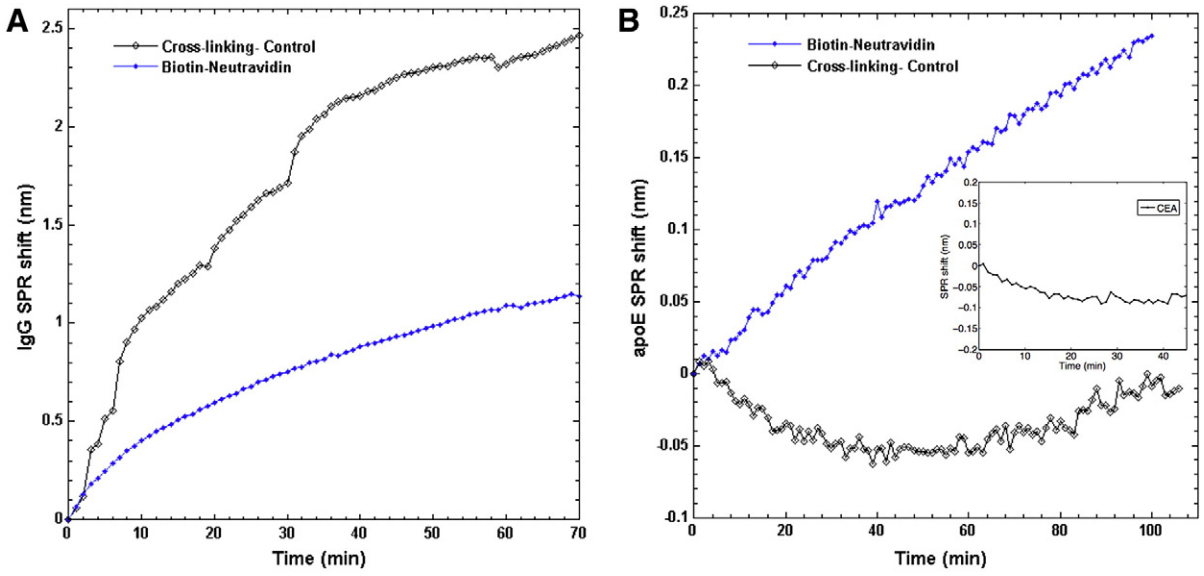

Figure 3. **(A)** Kinetic measurement of the SPR response for antibody immobilization for the *cross-linking* approach (black line), and for the *biotin–neutravidin* approach (blue line). **(B)** Kinetic measurement of the SPR response for 30 μg/mL human apoE sensing for the two functionalization strategies: apoE is not detectable with the *cross-linking* strategy (black line), while it is clearly visible using the *biotin–neutravidin* approach (blue line). Inset: SPR response upon exposure of CEA protein to the surface modified with *biotin–neutravidin* approach.

tetrameric biotin-binding protein, was then exposed to the biotinylated surface, and because of its affinity to biotin, immobilized onto the surface. Note that the dissociation constant of the pairs biotin/neutravidin is $K_D \sim 10^{-15}$ M, making it one of the strongest non-covalent bonds known.[19] Furthermore, using a biotin-coated sensing region instead of depositing directly neutravidin onto the sensor surface[25] enables to promote a specific orientation of the neutravidin and therefore of the subsequent biotinylated antibodies which is quite unlikely otherwise. In Figure 2, *C* is shown the measured shift of the SPR signal overtime, upon exposure of neutravidin to the biotinylated surface. The flow was kept constant at 10 μL/min to avoid depletion of the neutravidin concentration around the sensing area. From the SPR shift shown in Figure 2, *C*, and using known information regarding the sensor's sensitivity, the amount of neutravidin immobilized on the sensor can be estimated, as explained in Adsorbate quantification. Substituting in Eq. 1 the SPR shift of 3.5 nm (taken from Figure 2, *C*), the effective refractive index can be calculated to be $n_{eff} = 1.341$, and then used to estimate the penetration depth at the wavelength of 550 nm, from Eq. 2, giving a probe depth $l_d \sim 165$ nm. Assuming a refractive index of 1.45 for bulk neutravidin (a typical value for biomolecules[26]), from Eq. 3 the adsorbate layer thickness is calculated to be $d \sim 3.5$ nm, which corresponds well to the physical thickness of neutravidin (5.6 nm × 5 nm × 4 nm).[27] This result corroborates the hypothesis that a full monolayer of neutravidin has been deposited on the surface. In terms of surface coverage, a value of 400 ng/cm^2 is obtained from Eq. 4, which is consistent with data obtained in literature for a densely pack monolayer.[28]

After the immobilization of neutravidin on the surface, biotinylated antibodies are loaded into the sensor and bound to available neutravidin groups, taking advantage of the biotin function (see Figure 3, *A*, blue line), preventing any cross-binding of the antibodies to themselves, and thus linking the antibodies to the surfaces in a more ordered fashion. As for neutravidin, the quantity of biotinylated antibodies linked to the surface could be estimated from the SPR response, giving a surface coverage of 155 ng/cm^2 (assuming that the antibodies have the same refractive index and bulk density as for neutravidin), corresponding to approximately one immobilized antibody for each eight neutravidins, roughly half of that obtained with the *cross-linking* strategy (see Direct cross-linking).

Direct cross-linking

Considering the abundance of carboxylic groups in biological species, the *cross-linking* strategy is a convenient approach to immobilize proteins onto a surface, and this approach has been used for antibodies.[18] The main drawback of this approach is the cross-reactivity between amine and carboxylic groups present on other antibodies, resulting in antibodies cross-linking, which is itself quite undesirable because it could cause a loss of specificity and reactivity of the IgG binding sites. Additionally the immobilized antibodies will most likely be covalently bound with a random orientation which will further affect their ability to capture their antigen counterparts. Moreover, in the *cross-linking* approach, the SPR shift for antibodies is sensitive to the amount of cross-linking that occurs, and varies as a function of the relative concentration of antibodies and coupling reagents, which can raise issues of control and reproducibility of the reaction. In order to perform a reasonable comparison between the two different approaches, the concentrations of antibody solutions were fixed (Figure 3, *A*, black line). We believe that the step-wisely increase of the SPR response during the immobilization

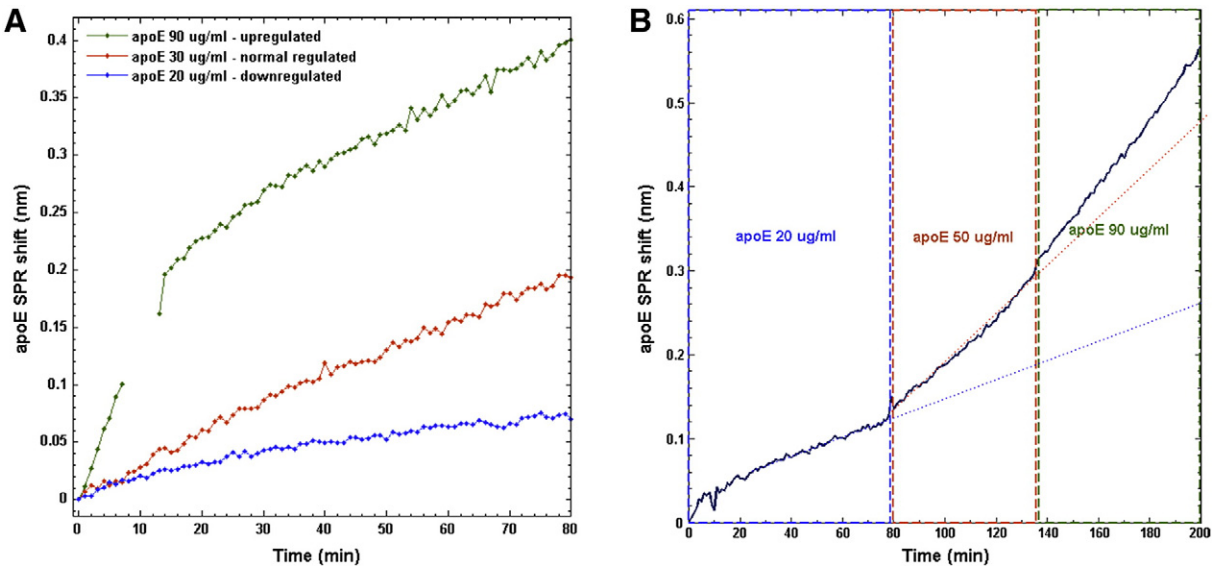

Figure 4. **(A)** Real-time measured SPR response for different concentrations of human apoE (down, normal and up-regulated): faster kinetics corresponds to higher concentrations. **(B)** Real-time measured SPR response for different concentrations of human apoE consecutively injected on the same sensor: the slope of the curve increases when higher concentrations are dosed.

of IgG in presence of EDC and NHS (Figure 3, *A*, black line) may be due to the binding of clusters of cross-linked antibodies with the surface.

The SPR shift for the *cross-linking* approach gives a surface coverage for the antibodies of approximately 305 ng/cm^2, twice that obtained by the biotin–neutravidin approach, as previously mentioned (see Biotin–neutravidin immobilization). This result could be easily explained by the cross-linking of the antibodies building up in a multilayer fashion, the only limit to this process being the life-time of the semi-stable amine-reactive NHS-ester, which at pH 7.4 is few hours.[18]

However, cross-linking of antibodies reduces their reactivity toward bait proteins and also, in the case of thick multilayer reduces chances for the protein to be captured within the probe depth.

apoE sensing

Figure 3, *B* shows the real-time measured SPR response for the two functionalization approaches upon the exposure of a 30-μg/mL solution (physiological range of regulation for humans[29]) of human apoE into the sensing region, flowed with a rate of 1 μL/min. The black line represents the SPR for the *cross-linking* approach, and no significative red shift is observed, meaning that the amount of apoE captured by the IgG is not detectable by our system. The blue line represents the SPR response for the case where the antibodies were linked accordingly to the *biotin–neutravidin* strategy. The binding kinetics obtained shows that 30 μg/mL apoE can be detected real time in a relatively short time (~1 h). Considering the small flow rate employed in the experiments, we expect to be in mass-transport limited conditions, resulting in slower binding kinetics respect to value reported in literature for typical specific binding between molecules.[30]

Note that in the *biotin–neutravidin* strategy the amount of IgGs immobilized on the sensor is half of that linked using the *cross-linking* approach, which demonstrates the importance of the order and orientation of the antibodies on the sensor surface. A negative control was performed in order to assure the specificity of the measure, exposing the protein carcino-embryonic antigen (CEA), and no shift of the SPR signal was observed (see inset in Figure 3, *B*).

Assuming that apoE has the same refractive index and bulk density as its antibodies and assuming that in the steady state each antibody binds two apoE proteins, we would expect the SPR response to be equivalent to a 39×2 kDa protein. Noting that the SPR shift for antibodies (which have a molecular weight of 150 kDa) is about 1.2 nm, and considering the case where apoE binds specifically to each IgG site available, a maximum shift of 0.6 nm would be expected. Therefore, we can estimate from the SPR response that after 1 h roughly 25% of the IgG binding sites are occupied.

Figure 3, *B* demonstrates the effect of different strategies to immobilize antibodies on the surface, and demonstrates that the *biotin–neutravidin* approach presented in this work, which enables improvements in the order and orientation of the IgGs, leads to significant performance improvements in the sensor.

apoE regulation

A point-of-care biosensor should be able not only to detect specifically one or more biomarkers, but it also must be able to provide quantitative information about their regulation, as in the typical samples biomarkers are present in physiological conditions. For example, in the case of apoE the normal regulation range in humans is 23–49 μg/mL,[29] with higher concentrations having been shown to be related to gastric cancer, where typically a 2.5-fold increase of apoE in serum occurs in

affected patients (unpublished results). The quantification of the amount of analyte present in the solution is not trivial, as it requires calibration of the real-time sensor response to different analyte concentrations.

The measured SPR response for different concentrations of apoE is shown in Figure 4, *A*, where each curve represents the binding kinetics of apoE in a single experiment. Three different concentrations are reported: 20, 30 and 90 μg/mL, respectively representing the down-regulated, normally regulated and up-regulated conditions for apoE in humans. From the data represented in Figure 4, *A* a discernment between different regulations is possible in a relatively short time frame (~1 h), and in particular for the case of the up-regulated condition, which could contribute to a gastric cancer diagnosis. The missing data point in Figure 4, *A*, for the case of up-regulated apoE is due to a false reading caused by an air bubble passing thought the sensor microfluidic flow cell.

According to the LOD estimated above and from the result shown in Figure 4, *A*, we believe the sensor to be able to detect a minimum apoE concentration between 5 and 10 μg/mL. Although this is not as sensitive as ELISA analysis (see technical notes from Mabtech about "*ELISA for Human Apolipoprotein E*," http://www.mabtech.com), we designed the sensor to work for the biological relevant regulation range for the biomarker.

Figure 4, *B* shows the measured SPR response, where different human apoE concentrations are exposed to the sensor within the same experiment, consecutively. The figure clearly demonstrates the different binding rapidity when higher concentrations of apoE are dosed, consistent with the data shown in Figure 4, *A*. Furthermore, Figure 4, *B* which shows the kinetic of the SPR signal when increasing concentration of the apoE is injected into the sensor flow cell, demonstrates that the discrimination of different concentrations of apoE can be performed within a single experiment. These results show that the analysis of the regulation of human apoE solutions is possible with the platform here proposed, and particularly that this system works for apoE concentrations that are clinically relevant in discriminating gastric cancer patients from unaffected individuals.

Discussion

In summary, a novel radiative-SPR platform, which was previously demonstrated for use in the rapid detection of the influenza A virus, is here proven to be effective for the detection in a relatively short timeframe (~1 h) of proteins with relatively low molecular weights in clinically relevant concentrations, as human apoE, that was discovered as a potential biomarker for gastric cancer in a proteomics study based on a genetically distinct mouse model and translated into humans. The importance of the surface functionalization approach is also demonstrated, showing that the antibody orientation plays a predominant role in the capture efficiency and consequently on the sensor ability to detect this small proteins. Although the quantity of antibodies immobilized with the *biotin–neutravidin* approach is half of that immobilized with the *cross-linking* strategy, only the *biotin–neutravidin* approach enabled the detection of a 30 μg/mL solution of apoE. This approach may offer significant advantages compared to protein A surface functionalization strategies such as a reduced reactivity with free IgG antibodies in clinical samples. We believe this strategy to be of general interest and not only related to this scattered surface plasmon based architecture. In fact, the *biotin–neutravidin* functionalization approach could be used with any biosensor, regardless of the transduction mechanism involved. The advantages are a better orientation of the immobilized antibodies onto the sensor's surface and the possibility of controlling the resulting surface density of immobilized antibodies.

Furthermore, the system has proven efficient also in quantifying the regulation of human apoE, being able to discern between physiological and gastric cancer conditions in a short timeframe, and has demonstrated to hold the needed qualities for point-of-care diagnostics.

Acknowledgments

The author thank Mr. R. Kostecki and Ms. R. Moore for sensor fabrications and Mr. A. Dowler for the flow cell fabrication.

References

1. Dostalek J, Ctyroky J, Homola J, Brynda E, Skalsky M, Nekvindova P, et al. Surface plasmon resonance biosensor based on integrated optical waveguide. *Sensors and Actuators B-Chemical* 2001;**76**(1-3):8-12.
2. Fan XD, White IM, Shopova SI, Zhu HY, Suter JD, Sun YZ. Sensitive optical biosensors for unlabeled targets: a review. *Anal Chim Acta* 2008;**620**(1-2):8-26.
3. Salamon Z, Macleod HA, Tollin G. Coupled plasmon-waveguide resonators: a new spectroscopic tool for probing proteolipid film structure and properties. *Biophys J* 1997;**73**(5):2791-7.
4. Jorgenson RC, Yee SS, Johnston KS, Compton BJ. A novel surface-plasmon resonance based fiber optic sensor applied to biochemical sensing. *Proceedings of Fiber Optics Sensors in Medical Diagnostics* 1993;**1886**:35-48.
5. Leung A, Shankar PM, Mutharasan R. A review of fiber-optic biosensors. *Sensors and Actuators B-Chemical* 2007;**125**(2):688-703.
6. Liedberg B, Lundstrom I, Stenberg E. Principles of biosensing with an extended coupling matrix and surface-plasmon resonance. *Sensors and Actuators B-Chemical* 1993;**11**(1-3):63-72.
7. Abbas A, Linman MJ, Cheng QA. New trends in instrumental design for surface plasmon resonance-based biosensors. *Biosens Bioelectron* 2011;**26**(5):1815-24.
8. Sharma AK, Jha R, Gupta BD. Fiber-optic sensors based on surface plasmon resonance: a comprehensive review. *Ieee Sensors Journal* 2007;**7**(7-8):1118-29.
9. François A, Boehm J, Oh SY, Kok T, Monro TM. Collection mode surface plasmon fibre sensors: a new biosensing platform. *Biosens Bioelectron* 2011;**26**(7):3154-9.
10. Corder EH, Saunders AM, Risch NJ, Strittmatter WJ, Schmechel DE, Gaskell PC, et al. Protective effect of apolipoprotein-E type-2 allele for late-onset Alzheimer-disease. *Nat Genet* 1994;**7**(2):180-4.
11. Chen JL, Li QQ, Wang JJ. Topology of human apolipoprotein E3 uniquely regulates its diverse biological functions. *Proc Natl Acad Sci U S A* 2011;**108**(36):14813-8.
12. Sakashita K, Tanaka F, Zhang X, Mimori K, Kamohara Y, Inoue H, et al. Clinical significance of ApoE expression in human gastric cancer. *Oncol Rep* 2008;**20**(6):1313-9.
13. Oue N, Hamai Y, Mitani Y, Matsumura S, Oshimo Y, Aung PP, et al. Gene expression profile of gastric carcinoma: identification of genes and tags potentially involved in invasion, metastasis, and carcinogenesis by serial analysis of gene expression. *Cancer Res* 2004;**64**(7):2397-405.

14. Boehm J, Francois A, Ebendorff-Heidepriem H, Monro TM. Chemical deposition of silver for the fabrication of surface plasmon microstructured optical fibre sensors. *Plasmonics* 2011;**6**(1):133-6.
15. White IM, Fan XD. On the performance quantification of resonant refractive index sensors. *Opt Express* 2008;**16**(2):1020-8.
16. Jung LS, Campbell CT, Chinowsky TM, Mar MN, Yee SS. Quantitative interpretation of the response of surface plasmon resonance sensors to adsorbed films. *Langmuir* 1998;**14**(19):5636-48.
17. Lukosz W. Principles and sensitivities of integrated optical and surface-plasmon sensors for direct affinity sensing and immunosensing. *Biosens Bioelectron* 1991;**6**(3):215-25.
18. Hermanson GT. Bioconjugate techniques. Rockford, Illinois: Academic Press; 1996.
19. Laitinen OH, Hytonen VP, Nordlund HR, Kulomaa MS. Genetically engineered avidins and streptavidins. *Cell Mol Life Sci* 2006;**63**(24): 2992-3017.
20. Homola J. Surface plasmon resonance sensors for detection of chemical and biological species. *Chem Rev* 2008;**108**(2):462-93.
21. Shevchenko Y, Francis TJ, Blair DAD, Walsh R, DeRosa MC, Albert J. In situ biosensing with a surface plasmon resonance fiber grating aptasensor. *Anal Chem* 2011;**83**(18):7027-34.
22. Pollet J, Delport F, Janssen KPF, Jans K, Maes G, Pfeiffer H, et al. Fiber optic SPR biosensing of DNA hybridization and DNA–protein interactions. *Biosens Bioelectron* 2009;**25**(4):864-9.
23. Yanase Y, Araki A, Suzuki H, Tsutsui T, Kimura T, Okamoto K, et al. Development of an optical fiber SPR sensor for living cell activation. *Biosens Bioelectron* 2010;**25**(5):1244-7.
24. Brian B, Sepulveda B, Alaverdyan Y, Lechuga LM, Kall M. Sensitivity enhancement of nanoplasmonic sensors in low refractive index substrates. *Opt Express* 2009;**17**(3):2015-23.
25. Peluso P, Wilson DS, Do D, Tran H, Venkatasubbaiah M, Quincy D, et al. Optimizing antibody immobilization strategies for the construction of protein microarrays. *Anal Biochem* 2003;**312**(2):113-24.
26. Fauchet PM, Miller BL, DeLouise LA, Lee MR, Ouyang H. In: Pavesi L, Fauchet PM, editors. *Biophotonics*. Berlin, Germany: Springer; 2008. p. 101-24.
27. Pugliese L, Coda A, Malcovati M, Bolognesi M. 3-Dimensional structure of the tetragonal crystal form of egg-white avidin in its functional complex with biotin at 2.7-Angstrom resolution. *J Mol Biol* 1993;**231**(3):698-710.
28. Cui XQ, Pei RJ, Wang XZ, Yang F, Ma Y, Dong SJ, et al. Layer-by-layer assembly of multilayer films composed of avidin and biotin-labeled antibody for immunosensing. *Biosens Bioelectron* 2003;**18**(1):59-67.
29. Mahley RW, Weisgraber KH, Huang YD. Apolipoprotein E: structure determines function, from atherosclerosis to Alzheimer's disease to AIDS. *J Lipid Res* 2009;**50**:S183-8.
30. Rich RL, Cannon MJ, Jenkins J, Pandian P, Sundaram S, Magyar R, et al. Extracting kinetic rate constants from surface plasmon resonance array systems. *Anal Biochem* 2008;**373**(1):112-20.